Microchimica Acta
https://doi.org/10.1007/s00604-018-2944-x

ORIGINAL PAPER

An organic electrochemical transistor for determination of microRNA21 using gold nanoparticles and a capture DNA probe

Jing Peng[1] · Tao He[1] · Yulian Sun[1] · Yawen Liu[1] · Qianqian Cao[1] · Qiong Wang[1,2] · Hao Tang[1]

Received: 22 April 2018 / Accepted: 2 August 2018

Abstract

A method is described for the determination of microRNA. It is based on the use of organic electrochemical transistors (OECTs) fabricated on a flexible poly(ethylene terephthalate) substrate. A gold electrode was modified with gold nanoparticles to immobilize the capture DNA probe and then served as the gate of the device. The detection of microRNA21 was realized by monitoring the change of the drain-source current after hybridization of capture DNA with microRNA21. Under optimal conditions, this biosensor exhibits good sensitivity and specificity. It works in the 5 pM to 20 nM microRNA concentration range and has a 2 pM detection limit.

Keywords Organic bioelectronics · Screen-printing · Flexible device · Nanomaterial surface modification · Self-assembling · Electrochemical biosensor · HeLa cells

Introduction

MicroRNAs, being a large family of endogenous and small noncoding RNAs, have attracted tremendous interests ranged from biology to biomedicine. More and more evidences demonstrate that microRNAs can be used as biomarkers in clinical diagnosis or targets in drug discovery, providing good potentials for cancer and other disease therapy [1]. To fully understand the role of microRNAs and further expand their potential applications, it should be very important to determine the microRNA expression level sensitively and accurately. The northern blot and reverse transcription polymerase chain reaction (RT-PCR) [2] are the most commonly used techniques and the gold standard for microRNA determination. These techniques present intrinsic advantages, for example, high sensitivity, specificity and precision; however, also have some limitations. Generally, these techniques involve relatively complicated processes and need various reagents or labels, which may be time-consuming and cost expensive. Some other techniques based on fluorescence [3], chemiluminescence [4], surface plasmon resonance (SPR) [5], surface-enhanced roman spectroscopy (SERS) [6] and electrochemistry [7, 8] have been developed for microRNA detection. Although great progress has been achieved, new methods and devices with high sensitivity for microRNA determination are still highly desired.

Organic electrochemical transistors (OECTs), being one kind of organic thin film transistors, have attracted great attentions in biosensors, bioelectronics and nanomedicines [9]. In contrast to the inorganic semiconductor (such as silicon)-based field effect transistors, the transistor device using organic semiconducting materials has shown several interesting characteristics including low temperature processing, oxide-free interfaces with aqueous electrolytes and "soft" mechanical property [10]. OECTs combine the advantages of organic semiconducting materials and the intrinsic feature of transistors for signal amplification. In transistors, the current flowing through source and drain electrodes can be modulated by a small variation of current or voltage in gate electrode. This signal amplification mechanism provides greater sensitivity in electronic devices. Moreover, the OECT device can be operated in aqueous solution at low voltages (< 1 V), making the

Electronic supplementary material The online version of this article (https://doi.org/10.1007/s00604-018-2944-x) contains supplementary material, which is available to authorized users.

✉ Hao Tang
tanghao@hunnu.edu.cn

[1] Key Laboratory of Chemical Biology and Traditional Chinese Medicine Research (Ministry of Education), College of Chemistry and Chemical Engineering, Hunan Normal University, Changsha 410081, People's Republic of China

[2] College of Science, Central South University of Forestry and Technology, Changsha 410004, People's Republic of China

Published online: 10 August 2018

interface between the biomolecules and electronics straightforward. The OECT-based biosensors have been developed for determination of glucose [11–13], dopamine [14], DNA [15], antigen [16], mammalian cells [17, 18] and etc. [19]. These studies suggest that the biosensors based on OECTs have excellent analytical performances.

Inspired by the above facts, we prepared a highly sensitive microRNA biosensor based on the OECTs. The screen-printed carbon electrodes on flexible poly(ethylene terephthalate) (PET) substrate are used as the source and drain electrodes; the DNA capture probe and gold nanoparticle (Au NP) modified Au electrode is served as the gate electrode (Fig. 1). Concerning the fabrication of OECT device, the Au or Pt electrodes are usually prepared by photolithography and used as the source and drain electrodes. Comparatively, screen-printing is a kind of high-throughput techniques. The screen-printed carbon electrodes have shown good potential for electrochemical sensors [20]. Therefore, the use of screen-printed carbon electrodes as the source and drain electrodes of OECTs may be suitable for mass production of cost-effective and disposable OECT devices. The detection of microRNAs using the OECT device is based on the change of drain-source current (I_{DS}) consequent to the hybridization between the target microRNA and the complementary DNA capture probe. The Au NPs are used because they have unique physical and chemical properties including good conductivity, large specific surface area, excellent electrochemical performance and good biocompatibility. Through the strong interaction of Au-S bond, biomolecules can be immobilized onto the Au NP surface with high efficiency. Taking these advantages, various kinds of biosensors based on Au NPs have been developed [21]. The modification of Au gate electrode with Au NPs may enhance the immobilization of DNA capture probes. Combined the signal amplification of OECTs with the efficient immobilization of DNA capture probes, the microRNA biosensor based on OECTs will have improved analytical performances. As a model case, microRNA21 is used as the target, which plays important role in development of heart disease [22]. The OECT-based microRNA21 biosensor exhibits good analytical properties (high sensitivity, low detection limit and good selectivity) for microRNA21 determination.

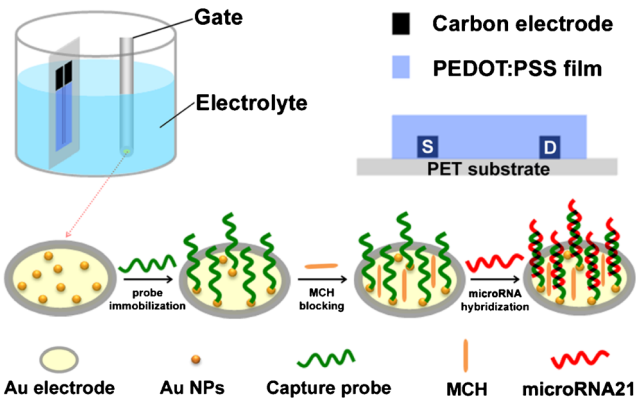

Fig. 1 Schemes demonstrating the principle of microRNA21 biosensor based on OECTs

Materials and methods

Chemicals and instruments

The synthetic 5′-thiol group terminated DNA capture probe, microRNA21, microRNA24, and microRNA29 were obtained from Invitrogen Corporation (www.thermofisher.com). The base sequences of DNA capture probe and microRNAs are as follows:

DNA probe: 5'-HS-T CAA CAT CAG TCT GAT AAG CTA-3'
microRNA21: 5'-UAG CUU AUC AGA CUG AUG UUG A-3'
microRNA24: 5'-UGG CUC AGU UCA GCA GGA ACA G-3'
microRNA29: 5'-UAG CAC CAU CUG AAA UCG GUU A-3'

The total RNA samples were extracted from cultured human cervical cancer (HeLa) cells by TRIZOL reagents (Invitrogen Corporation, www.thermofisher.com) according to the manufacturer's recommended protocol. The quality of total RNA was routinely assessed by gel electrophoresis (1% gelose, 170 V, 20 min) and BioPhotometer plus (Eppendorf, www.eppendorf.com). The 5S rRNA, 18S rRNA and 28S rRNA bands are all clear in the electrophoresis picture (**Fig. S1**, Electronic Supplementary Material) and the OD_{260}/OD_{280} is larger than 1.8 (the results not shown), suggesting that high quality and intact RNA is obtained from the cell samples. The total concentration was measured by UV-vis spectrophotometry. HeLa cells were purchased from Cancer Research Institute of Xiangya Medical College. UltraPure diethyl pyrocarbonate (DEPC)-treated water was purchased from Invitrogen Corporation (www.thermofisher.com). The DEPC-treated water was used for the microRNA21 determination and preparation of total RNA sample solution (1.0 μg μL^{-1}). Conductive carbon ink (Electrodag 581SS) was obtained from Henkel Adhesive Technologies (www.henkel-adhesives.com). Poly-(3,4-ethylenedioxythiophere):poly-(styrene sulfonic acid) (PEDOT:PSS) aqueous solution (Clevios™ PH 1000) was purchased from Heraeus (www.heraeus.com) and stored at 4 °C for future use. Dimethyl sulfoxide (DMSO) was obtained from Sinopharm Chemical Reagent Co. Ltd. (www.sinoreagent.com). Chloroauric acid hydrate (analytical grade) was purchased from Shanghai Chemical Reagent Co., Ltd. (www.srici-fc.com). 6-

mercapto-1-hexanol (MCH) was purchased from J&K Scientific Ltd. (www.jkchemical.com). Phosphate buffered saline (PBS, 0.1 M, pH 7.38; containing 8.0 g L^{-1} NaCl and 0.2 g L^{-1} KCl) was used in the experiments. Isopropyl alcohol, acetone, ethanol and all other reagents were of analytical grade or better. Milli-Q ultrapure water (> 18 MΩ cm, Milli-pore Co., Ltd.) and freshly prepared solutions were used throughout.

The CHI 1040B bipotentiostat (CH Instruments Co., www.chinstruments.com) was used for OECT device characterization and microRNA21 determination. The CHI 660C electrochemical workstation (CH Instruments Co., www.chinstruments.com) and a conventional three-electrode system were used in the electrochemical experiments. The DNA capture probe modified Au NP/Au electrodes (Au diameter 3 mm) were served as the gate or working electrodes. The reference electrode was KCl-saturated calomel electrode (SCE) and the platinum wire electrode was used as the counter electrode. For the electrochemical experiments, all potential values given below were referred to the SCE. The experiments were performed at room temperature and the measurements were repeated at least three times. The means of measurements were presented with the standard deviations (SD). The screen-printer (AT-25PA, ATMA TUNG YUAN M/C Ind. Co., Ltd., www.atma-usa.com) was used to fabricated the carbon source and drain electrodes of the OECT device. The vacuum spin-coater (VTC 100, Shenyang Kejing Auto-instrument Co., Ltd., www.sykejing.com) was used to prepare the PEDOT:PSS-based channel. The micromorphology of Au NPs was characterized by scanning electron microscopy (SEM, JSM 5600 LV, operating at 20 kV; www.jeolusa.com).

Preparation of the OECT devices and MCH/probe/Au NP/Au electrodes

The OECT device architecture is shown in Fig. 1. The OECTs based on the PEDOT:PSS active layer and the screen-printed carbon electrodes were fabricated according to procedures [23] described in the Electronic Supplementary Material.

Before Au NP modification and DNA capture probe immobilization, the Au electrode was pretreated according to a well-established procedure (see Electronic Supplementary Material). For the preparation MCH/probe/Au NP/Au electrode, the Au NPs were first electrodeposited on the pretreated Au electrode in 0.5 M H_2SO_4 aqueous solution containing 3.0 mM $HAuCl_4$. The electrodeposition potential and time are −0.2 V (vs. SCE) and 500 s. After rinsed with copious ultrapure water, 10 μL of DNA probe (1.0 μM) PBS solution were drop-coated onto the surface of Au NP/Au electrode, followed by self-assembling for 12 h under heliophobe condition. The probe/Au NP/Au electrode was carefully rinsed with PBS solution. To decrease the nonspecific adsorption of DNA probes and block the active surface of the Au NP/Au electrode [24], the electrode was then immersed into 100 μL of MCH aqueous solution (5 mM) for 2 h. After carefully rinsed with PBS, the MCH/probe/Au NP/Au electrode was used for the following measurements. For comparisons, the probe/Au and MCH/probe/Au electrodes were also prepared by the same processes as described above.

OECT characterization and electrochemical measurements

The OECT devices were characterized by using a controlled bipotentiostat (CHI 1040B, CH Instruments Co., www.chinstruments.com) in a small beaker filled with PBS (0.1 M, pH 7.38). Various electrodes including the bare Au and Au NP/Au electrodes were used as the gate electrodes. The output characteristic of the OECT device was investigated at a fixed gate-source voltage (V_{GS}, 0, 0.2, 0.4, 0.6, 0.8, and 1.0 V) and a continuous scanning of drain-source voltage (V_{DS}, 0 to −0.4 V, scan rate, 10 mV s^{-1}). The transfer property of the OECT device was measured at a fixed V_{DS} (−0.2 V) and a continuous scanning of V_{GS} from 0 to 1.0 V (scan rate, 10 mV s^{-1}). The working principle of microRNA21 determination by PEDOT:PSS-based OECTs is schemed in Fig. 1. The OECT device was tested at a fixed V_{DS} = −0.2 V and a constant (optimized at 0.6 V) gate voltage, and the I_{DS} vs. time plot was recorded. The specific interaction of target microRNA21 with the DNA capture probe that immobilized on the Au NP/Au gate electrode generates potential variation at the interface of gate electrode/electrolyte solution, leading to the change of I_{DS}. The detection of microRNA21 in total RNA sample is based on the same principle.

The electrochemical impedance spectroscopy (EIS) was used to characterize the interface properties of various electrodes including the bare Au, probe/Au, MCH/probe/Au, and probe/Au NP/Au electrodes. The EIS measurements were conducted in PBS (0.1 M, pH 7.38) containing 2.0 mM $[Fe(CN)_6]^{3-/4-}$ redox probe. The impedance data was recorded at the open circuit potential in the ac frequency range from 100 kHz to 0.01 Hz with an excitation signal of 5 mV. The impedance, Z, is expressed in term of its real (Z') and imaginary ($-Z''$) components. The data from the electrochemical impedance measurements were analyzed by the software of CHI 660C electrochemical workstation.

The open circuit potential of the MCH/probe/Au NP/Au electrode was measured in the stirred PBS (0.1 M, pH 7.38) using a two-electrode cell system. The MCH/probe/Au NP/Au electrode was used as the working electrode and a SCE electrode was served as the reference electrode. The change in open circuit potential (ΔE) before and after the addition of microRNA21 was recorded as a function of time.

Results and discussion

Characterization of the OECT device and MCH/probe/Au electrode

The typical output characteristic of the OECT device using the bare Au gate electrode is shown in **Fig. S2** (Electronic Supplementary Material). The OECT device exhibits satisfied I_{DS} modulation in the studied V_{DS} and V_{GS} range. For example, at V_{GS} = 1.0 V, the device achieves saturation regime at about V_{DS} = −0.2 V. The MCH/probe/Au electrode was characterized by cyclic voltammetry (CV) and EIS. The results (**Fig. S3**, Electronic Supplementary Material) demonstrate the successfully preparation of the microRNA21 sensing interface at the Au gate electrode.

Optimization of method

The following parameters were optimized: (a) probe concentration; (b) probe assembling time; (c) MCH concentration; (d) MCK blocking time. Respective data and Figures are given in the Electronic Supplementary Material (**Fig. S4**). The following experimental conditions were found to give best results: (a) best probe concentration: 1.0 μM; (b) optimal assembling time: 12 h; (c) best MCH concentration: 5 mM; (d) best MCH blocking time: 2 h.

Improved probe immobilization and OECT responses by Au NP modification

Figure 2a shows the SEM image of the Au NP/Au electrode. The electrodeposited Au NPs are almost monodispersive on the Au electrode surface. The size of Au NPs is ~ 50 nm. The effects of Au NP modification on the DNA capture probe immobilization and OECT responses were investigated. In contrast to bare Au gate electrode (Fig. 2b, black line), the transfer plot of the OECT device using the Au NP/Au gate electrode (Fig. 2b, red line) shifts horizontally to lower gate voltage for about 48 mV. The Au NP modification renders the Au NP/Au gate electrode larger specific surface area, leading to more sensitive I_{DS} modulation in OECTs. More importantly, the electron transfer resistance (R_{ct}) of probe/Au NP/Au electrode (Fig. 2c, red line) is greatly larger than that of the probe/Au electrode (Fig. 2c, black line), suggesting the Au NP modification can improve the DNA capture probe immobilization. Consequently, the OECT device using the Au NP modified gate electrode will have more sensitive response to microRNA21. Figure 2d shows the typical responses of the OECT devices to addition of microRNA21. To compare the responses of different OECTs, the $I_{DS}/I_{DS,0}$ or normalized current response (NCR) is used. The NCR is calculated according the following equation: $NCR = \left|\frac{I_{DS}-I_{DS,0}}{I_{DS,0}}\right|$, where $I_{DS,0}$ and I_{DS} is the channel current before and after an addition of microRNA21 at concentration of interest. The interaction

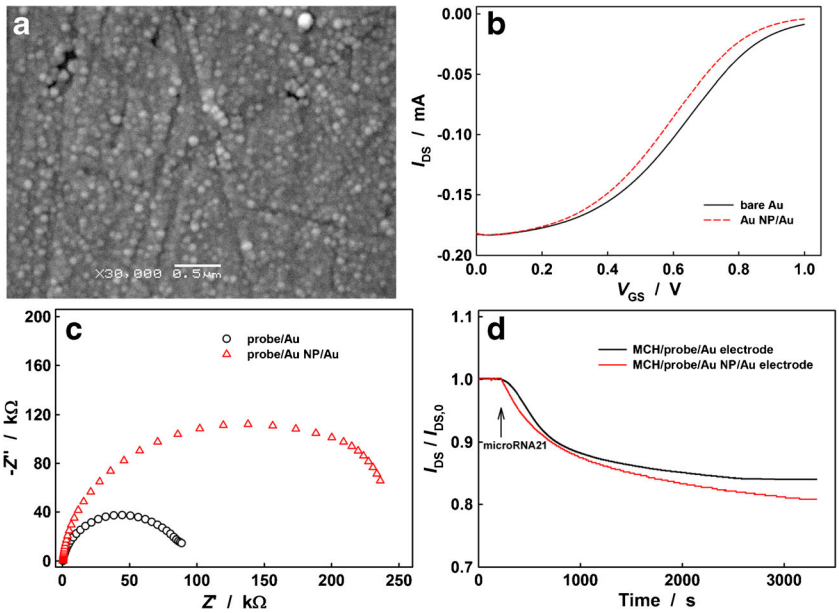

Fig. 2 **a** SEM image of the Au NP/Au electrode. **b** The transfer characteristics of OECT devices using the bare Au (black line) or Au NP/Au (red line) gate; PBS (pH 7.38) as the electrolyte; V_{DS} = −0.2 V and V_{GS} scan rate is 0.01 V s^{-1}. **c** The Nyquist plots of the probe/Au (black line) and probe/Au NP/Au (red line) electrodes in PBS (pH 7.38) solution containing 2.0 mM $[Fe(CN)_6]^{3-/4-}$. **d** The normalized responses of OECT devices to addition of microRNA21; the MCH/probe/Au (black line) or MCH/probe/Au NP/Au (red line) electrode as the gate; PBS (pH 7.38) as the electrolyte; V_{DS} = −0.2 V and V_{GS} = 0.6 V. The electrodeposition time of Au NPs is 500 s; the microRNA21 concentrations are 80 nM (for MCH/probe/Au gate electrode) and 20 nM (for MCH/probe/Au NP/Au gate electrode)

between the added microRNA21 and immobilized capture probes leads to the decrease of I_{DS} (Fig. 2d). The I_{DS} becomes stable after about 50 min, suggesting that the interaction reaches a dynamic balance. The I_{DS} change of the OECT device using the MCH/probe/Au NP/Au gate electrode (Fig. 2d, red line) is larger than that using the MCH/probe/Au gate electrode (Fig. 2d, black line), even when the microRNA21 concentration is 4 times as large as that in the case of using MCH/probe/Au NP/Au gate. This demonstrates that the improved current modulation and probe immobilization by Au NP modification can greatly enhance the sensitivity of the OECT-based microRNA21 biosensor.

The change of I_{DS} upon addition of microRNA21 should be attributed to the change of the electrolyte solution potential (V_{sol}), which results from the formation of DNA capture probe-microRNA21 hybrids. V_{sol} is the potential acting on the OECT channel, and ultimately determines the OECT current modulation [25]. The MCH/probe/Au NP/Au electrode was used as the working electrode, and the open circuit potential (also referred as the equilibrium potential) of the MCH/probe/Au NP/Au electrode after addition of microRNA21 was monitored (**Fig. S5**, Electronic Supplementary Material). Although the open circuit potential is measured at which there is no current (no applied voltage), it can be used to characterize the potential change due to the capture probe-microRNA21 interaction at the gate/electrolyte interface. As shown in **Fig. S5** (Electronic Supplementary Material), the open circuit potential decreases with the addition of microRNA21, and the ΔE is about 30 mV. Therefore, it is considered that the probe-microRNA21 interaction leads to decrease of potential at gate/electrolyte interface, which means the increase of V_{sol}, and as a result, the I_{DS} decreases with the addition of microRNA21.

The electrodeposition time of Au NPs and applied V_{GS} were optimized. Respective data and Figures are given in the Electronic Supplementary Material (**Figs. S6-S7**). The following experimental conditions were found to give best results: (a) best electrodeposition time of Au NPs: 500 s; (b) optimal applied V_{GS}: 0.6 V.

Analytical performances for microRNA21 determination

The microRNA24 and microRNA29 were used as control to test the selectivity of the OECT-based biosensor. Figure 3a shows the NCR of OECT devices using the MCH/probe/Au NP/Au gate electrodes to different microRNAs. The NCR from the hybridization with microRNA24 or microRNA29 is very little in contrast to that from microRNA21, suggesting that the assay has good selectivity. Theoretically, the capture probe DNA would not hybridize with a non-complementary sequence. However, the nonspecific adsorption of microRNA24 or microRNA29 cannot be completely eliminated, which results in the little change of I_{DS}.

The reproducibility of the OECT-based biosensor for microRNA21 determination was also evaluated. Samples (50 nM) were detected by five OECT-based biosensors prepared under the same conditions, giving a relative standard deviation (RSD) of 11.7%. This reveals that the microRNA21 biosensor has satisfied reproducibility. The relative large RSD may be mainly due to the difference of the prepared OECT devices.

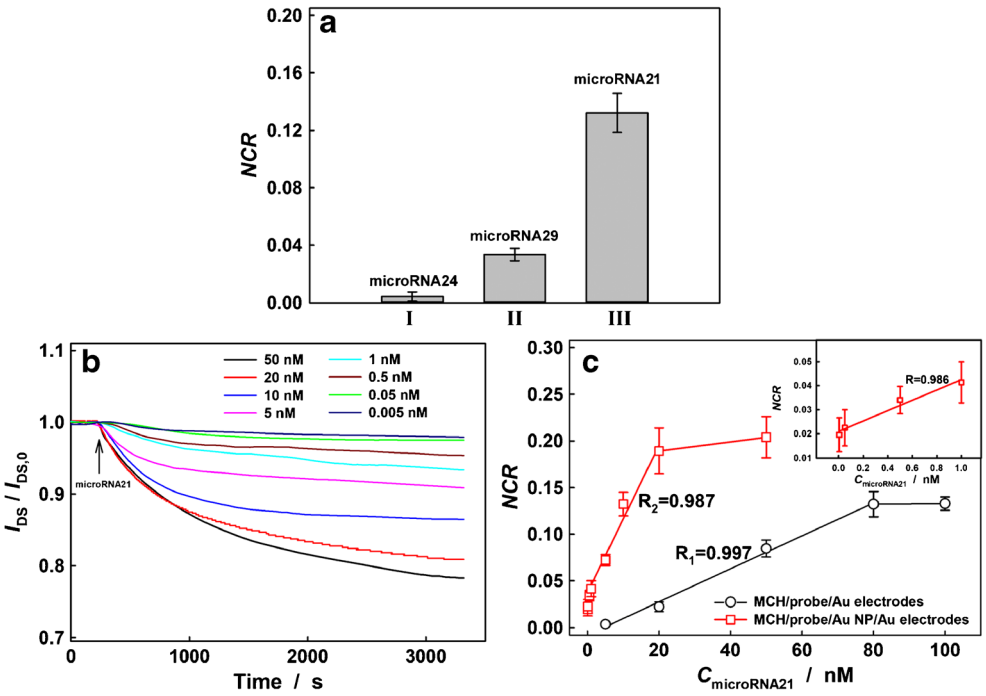

Fig. 3 **a** The NCR of OECT-based biosensor to microRNA21, microRNA24, and microRNA29; the concentrations of microRNAs are all 10 nM. **b** The normalized responses of OECT biosensors to different concentrations of microRNA21; the MCH/probe/Au NP/Au electrodes as the gate; PBS (pH 7.38) as the electrolyte; V_{DS} = −0.2 V and V_{GS} = 0.6 V. **c** The calibration plots of OECT-based microRNA21 biosensor using the MCH/probe/Au (black line) and MCH/probe/Au NP/Au gate (red line). Insert plot of Fig. 3c: enlarged calibration plot in the ~ 1 nM microRNA concentration range for the biosensor using the MCH/probe/Au NP/Au gate

Table 1 Summary of detection limit and linear range of microRNA biosensors reported in literatures

Amplification strategy	Detection method	Target microRNAs	Detection Limit	Linear range	References
Hairpin probes and Au NPs	Colorimetry	microRNA21	6.8 pM	20 pM - 10 nM	[26]
Metal dielectric nanostructured materials	SERS	microRNA222	485 pM	0.5–50 nM	[6]
DNA*RNA antibody	SPR	microRNA122	2 pM	10–100 pM	[5]
Electropolymerized polypyrrole-modified electrode	EIS	microRNA21	170 pM	No data	[27]
Enzyme amplified biosensing	Voltammetry	microRNA21	1 μM	No data	[28]
DNA-Au NP hybrids	Colorimetry	microRNA215	60 pM	No data	[29]
DNA generated electrochemical current coupled with HCR	Voltammetry	microRNA21	0.5 fM	1 fM - 1 nM	[32]
Target-triggered hybridization chain reaction	Voltammetry	microRNA21	33 aM	0.1 fM - 0.1 nM	[33]
Pd nanoparticles as enhancer and linker	Amperometry	microRNA155	1.87 pM	5.6 pM - 560 nM	[30]
MWCNTs/GC electrode	Voltammetry	microRNA24	1 pM	1 pM - 10 nM	[31]
MCH/probe/Au NP/Au electrode	OECTs	microRNA21	2 pM	5 pM - 20 nM	This work

Figure 3b shows the normalized responses ($I_{DS}/I_{DS,0}$) of OECT devices using the MCH/probe/Au NP/Au gate to different concentrations of microRNA21. The relationship between NCR and microRNA21 concentration ($C_{microRNA21}$) is presented in Fig. 3c. For the OECT devices using the MCH/probe/Au NP/Au gate (Fig. 3c, red line; insert plot of Fig. 3c), the NCR ~ $C_{microRNA21}$ plot exhibits two linear ranges with different slopes in the studied concentration range (5 pM to 20 nM). A flat value is observed when 50 nM of the target is used. The regression equations in the ranges of 5 pM - 1 nM and 1–20 nM can be obtained and expressed as $NCR = 0.021 + 0.022C_{microRNA21}$ and $NCR = 0.038 + 0.0079C_{microRNA21}$. The two linear plots have the slopes of 0.022 nM^{-1} and 0.0079 nM^{-1} (the sensitivity of the microRNA21 biosensor) and the correlation coefficients are 0.986 and 0.987. Similar result is obtained for the OECT devices using the MCH/probe/Au gate (Fig. 3c, black line), and the NCR exhibits linear range from 5 nM to 80 nM. The regression equation in the linear range can be obtained and expressed as $NCR = -0.0078 + 0.0017C_{microRNA21}$. The slope of the linear plot is 0.0017 nM^{-1} and the correlation coefficient is 0.997. The OECT device using the MCH/probe/Au NP/Au gate has greatly larger slope than that using the MCH/probe/Au gate, demonstrating the enhanced sensitivity for microRNA21 detection by the Au NP modification. A detection limit of 2 pM for the target microRNA21 can be estimated using 3σ (where σ is the standard deviation of the blank solution). This is lower than those using various sensing platforms including hairpin probes and Au NPs [26], metal-dielectric nanostructures [6], electropolymerized polypyrrole-modified electrode [27], labeled alkaline phosphatase [28], DNA-Au NP hybrids [29], and is comparable with those using other signal amplification [5, 30, 31], but is poor in contrast to those using the strategy of hybridization chain reaction [32, 33]. The detection limit and linear range of several kinds of biosensors for different microRNA determination are listed in Table 1. The analytical applicability of the OECT-based microRNA21 biosensor was evaluated by determination microRNA21 in the total RNA sample. The concentration of microRNA21 in the total RNA sample (extracted from HeLa cells) is found to be 9.2 nM ($n = 3$, RSD = 14.5%), which is comparable with that (9.65 nM, n = 3, RSD = 2.6%) obtained from the quantitative PCR detection. The results suggest that the OECT-based biosensor has good potential for complex microRNA sample detection.

Although the OECT device shows good analytical characteristics for microRNA21 determination, the MCH/probe/Au NP/Au gate is separated from organic active layer on the PET substrate, which is inconvenient for the device integration and miniaturization. In addition, the manual pre-treatment of Au electrode may be a factor that influences the reproducibility. Further studies on screen-printing of Au electrode on PET and enhancing of automation degree are needed to prepare all-printed OECTs. It would facilitate the integration of OECTs with other sensing system and improve reproducibility of the devices.

Conclusions

In summary, we have fabricated an OECT-based biosensor for microRNA21 detection using the Au NP and capture probe modified gate. By engagement of the intrinsic signal amplification of OECTs and greatly improved probe immobilization of Au NPs, this biosensor achieved microRNA21 determination with good sensitivity, selectivity and acceptable applicability in total RNA sample, which may find potential application in the routine microRNA bioanalysis. More research on all-printed OECTs with promoted automation degree will be carried out in the future. We also expect that the all-printed OECTs could

be used as disposable microRNA sensing device for clinical diagnostics and point of care service.

Acknowledgments This work was supported by the National Natural Science Foundation of China under grants (21275050 and 21145001), the Hunan Provincial Natural Science Foundation of China (13JJ1016), the Scientific Research Fund of Hunan Provincial Education Department (13A053), the Construct Program of the Key Discipline in Hunan Province, and Foundation of the Science & Technology Department of Hunan Province (2016SK2020).

Compliance with ethical standards The author(s) declare that they have no competing interests.

References

1. De Pontual L, Yao E, Callier P, Faivre L, Drouin V, Cariou S, Van Haeringen A, Genevieve D, Goldenberg A, Oufadem M, Manouvrier S, Munnich A, Vidigal JA, Vekemans M, Lyonnet S, Henrion-Caude A, Ventura A, Amiel J (2011) Germline deletion of the miR-17~92 cluster causes skeletal and growth defects in humans. Nat Genet 43:1026–1030
2. Chen C, Ridzon DA, Broomer AJ, Zhou Z, Lee DH, Nguyen JT, Barbisin M, Xu NL, Mahuvakar VR, Andersen MR, Lao KQ, Livak KJ, Guegler KJ (2005) Real-time quantification of microRNAs by stem-loop RT-PCR. Nucleic Acids Res 33:e179
3. Tu Y, Li W, Wu P, Zhang H, Cai C (2013) Fluorescence quenching of graphene oxide integrating with the site-specific cleavage of the endonuclease for sensitive and selective microRNA detection. Anal Chem 85:2536–2542
4. Bi S, Zhang J, Hao S, Ding C, Zhang S (2011) Exponential amplification for chemiluminescence resonance energy transfer detection of microRNA in real samples based on a cross-catalyst strand-displacement network. Anal Chem 83:3696–3702
5. Sípová H, Zhang S, Dudley AM, Galas D, Wang K, Homola J (2010) Surface plasmon resonance biosensor for rapid label-free detection of microribonucleic acid at subfemtomole level. Anal Chem 82:10110–10115
6. Chiadò A, Novara C, Lamberti A, Geobaldo F, Giorgis F, Rivolo P (2016) Immobilization of oligonucleotides on metal-dielectric nanostructures for miRNA detection. Anal Chem 88:9554–9563
7. Wu X, Chai Y, Zhang P, Yuan R (2016) An electrochemical biosensor for sensitive setection of microRNA-155: combining target recycling with cascade catalysis for signal amplification. ACS Appl Mater Interfaces 7:713–720
8. Miao X, Wang W, Kang T, Liu J, Shiu KK, Leung CH, Ma DL (2016) Ultrasensitive electrochemical detection of miRNA-21 by using an iridium(III) complex as catalyst. Biosens Bioelectron 86: 454–458
9. Strakosas X, Bongo M, Owens RM (2015) The organic electrochemical transistor for biological applications. J Appl Polym Sci 132:41735
10. Rivnay J, Owens RM, Malliaras GG (2014) The rise of organic bioelectronics. Chem Mater 26:679–685
11. Ji X, Lau HY, Ren X, Peng B, Zhai P, Feng SP, Chan PKL (2016) Highly sensitive metabolite biosensor based on organic electrochemical transistor integrated with microfluidic channel and poly(N-vinyl-2-pyrrolidone)-capped platinum nanoparticles. Adv Mater Technol 1:1600042
12. Liao C, Zhang M, Niu L, Zheng Z, Yan F (2013) Highly selective and sensitive glucose sensors based on organic electrochemical transistors with graphene-modified gate electrodes. J Mater Chem 1:191–200
13. Scheiblin G, Aliane A, Strakosas X, Curto VF, Coppard R, Marchand G, Owens RM, Mailley P, Malliaras GG (2015) Screen-printed organic electrochemical transistors for metabolite sensing. MRS Commun 5:507–511
14. Tang H, Lin P, Chan HL, Yan F (2011) Highly sensitive dopamine biosensors based on organic electrochemical transistors. Biosens Bioelectron 26:4559–4563
15. Pappa A-M, Inal S, Roy K, Zhang Y, Pitsalidis C, Hama A, Pas J, Malliaras GG, Owens RM (2017) Polyelectrolyte layer-by-layer assembly on organic electrochemical transistors. ACS Appl Mater Interfaces 9:10427–10434
16. Kim DJ, Lee NE, Park JS, Park IJ, Kim JG, Cho HJ (2010) Organic electrochemical transistor based immunosensor for prostate specific antigen (PSA) detection using gold nanoparticles for signal amplification. Biosens Bioelectron 25:2477–2482
17. Yao C, Li Q, Guo J, Yan F, Hsing IM (2015) Rigid and flexible organic electrochemical transistor arrays for monitoring action potentials from electrogenic cells. Adv Healthcare Mater 4:528–533
18. Khodagholy D, Doublet T, Quilichini P, Gurfinkel M, Leleux P, Ghestem A, Ismailova E, Hervé T, Sanaur S, Bernard C (2013) In vivo recordings of brain activity using organic transistors. Nat Commun 4:1575
19. Gualandi I, Marzocchi M, Scavetta E, Calienni M, Bonfiglio A, Fraboni B (2015) A simple all-PEDOT:PSS electrochemical transistor for ascorbic acid sensing. J Mater Chem B 3:6753–6762
20. Marquette CA, Lawrence MF, Blum LJ (2006) DNA covalent immobilization onto screen-printed electrode networks for direct label-free hybridization detection of p53 sequences. Anal Chem 78:959–964
21. Saha K, Agasti SS, Kim C, Li X, Rotello VM (2012) Gold nanoparticles in chemical and biological sensing. Chem Rev 112:2739–2779
22. Thum T, Gross C, Fielder J, Fischer T, Kissler S, Bussen M, Galuppo P, Just S, Rottbauer W, Frantz S, Castoldi M, Soutschek J, Koteliansky V, Rosenwald A, Basson MA, Licht JD, Pena JTR, Bauersachs J, Engelhardt S (2008) MicroRNA-21 contributes to myocardial disease by stimulating MAP kinase signalling in fibroblasts. Nature 456:980–984
23. Guo X, Liu J, Liu F, She F, Zheng Q, Tang H, Ma M, Yao S (2017) Label-free and sensitive sialic acid biosensor based on organic electrochemical transistors. Sensors Actuators B Chem 240:1075–1082
24. Shuai HL, Huang KJ, Chen YX, Fang LX, Jia MP (2017) Au nanoparticles/hollow molybdenum disulfide microcubes based biosensor for microRNA-21 detection coupled with duplex-specific nuclease and enzyme signal amplification. Biosens Bioelectron 89:989–997
25. Bernards DA, Macaya DJ, Nikolou M, DeFranco JA, Takamatsu S, Malliaras GG (2008) Enzymatic sensing with organic electrochemical transistors. J Mater Chem 18:116–120
26. Miao X, Ning X, Li Z, Cheng Z (2016) Sensitive detection of miRNA by using hybridization chain reaction coupled with positively charged gold nanoparticles. Sci Rep 6:32358
27. Kaplan M, Kilic T, Guler G, Mandli J, Amine A, Ozsoz M (2016) A novel method for sensitive microRNA detection: Electropolymerization based doping. Biosens Bioelectron 92:770–778
28. Kilic T, Topkaya SN, Ozkan Ariksoysal D, Ozsoz M, Ballar P, Erac Y, Gozen O (2012) Electrochemical based detection of microRNA, miR21 in breast cancer cells. Biosens Bioelectron 38:195–201
29. Gao X, Xu H, Baloda M, Gurung AS, Xu L-P, Wang T, Zhang X, Liu G (2014) Visual detection of microRNA with lateral flow nucleic acid biosensor. Biosens Bioelectron 54:578–584

30. Wu X, Chai Y, Yuan R, Su H, Han J (2013) A novel label-free electrochemical microRNA biosensor using Pd nanoparticles as enhancer and linker. Analyst 138:1060–1066
31. Li F, Peng J, Wang J, Tang H, Tan L, Xie Q, Yao S (2014) Carbon nanotube-based label-free electrochemical biosensor for sensitive detection of miRNA-24. Biosens Bioelectron 54:158–164
32. Feng K, Liu J, Deng L, Yu H, Yang M (2018) Amperometric detection of microRNA based on DNA-controlled current of a molybdophosphate redox probe and amplification via hybridization chain reaction. Microchim Acta 185:28–35
33. Liu H, Bei X, Xia Q, Fu Y, Zhang S, Liu M, Yang Y (2016) Enzyme-free electrochemical detection of microRNA-21 using immobilized hairpin probes and a target-triggered hybridization chain reaction amplification strategy. Microchim Acta 183:297–304